Early flutter warning in wind tunnel testing using Operational Modal Analysis

Peter Karkle, Mikhail Pronin*, Bart Peeters**, Raphaël Van der Vorst***
**Central Aerohydrodynamic Institute (TsAGI)*
1 Zhukovsky Street, Moscow Region, 140180, Russian Federation
***LMS International*
Interleuvenlaan 68, B-3001 Leuven, Belgium

Abstract

This paper discusses an early-warning system for flutter detection during wind tunnel testing of scaled models. In this type of testing, it is desired to carefully verify and track the vibration behavior, since during flutter appearance, model destruction may occur. To this aim, sensors are mounted on the model and the dynamic response is measured. From the analysis of the data, an assessment of flutter safety can be made. In this paper, wind tunnel data at various flow conditions are used to validate the speed and reliability of an Operational Modal Analysis approach for tracking the evolution of the eigenfrequencies, damping ratios and mode shapes of the tested component. Operational Modal Analysis allows extracting these parameters from the structural response to natural turbulence excitation without the need for special artificial excitation. Both strain gauge and acceleration data are used.

1. Introduction

The development cycle of a new aircraft consists of several modelling and testing stages: structural finite element (FE) modelling, ground vibration testing (GVT), computational fluid dynamics (CFD) modelling, wind tunnel testing, and in-flight tests (Figure 1). These flight (vibration) tests allow the validation of the analytical models under various real flight conditions and, more important, allow to assess the aero-elastic interaction, as a function of airspeed and altitude, between the structure and the aerodynamic forces as they may lead to a sudden unstable behaviour known as flutter. Flutter shows up in the vibration signals as apparent negative damping and corresponding sudden increase of the vibration amplitudes. For economic and safety reasons (i.e. to avoid a loss of the aircraft), it is evidently avoided that an aircraft goes into flutter during an in-flight test, but it has to be certified that it has sufficient flutter margin when flying at the different points of the flight envelope where it is designed for. To determine this margin, typically, the trends of eigenfrequencies and damping ratios of the critical modes as a function of airspeed are carefully studied. This explains the need to perform a modal analysis during the flight. More background information on flight flutter testing can be found in [1][2]. An overview and discussion of some interesting data-based and model-based approaches to predict the onset of flutter during flight testing can be found in [3][4][5].

When exciting the aircraft artificially during the flight, a reference signal representative for the force input is typically recorded, Frequency Response Functions (FRFs) can be estimated and classical modal analysis can be applied. Exciting the aircraft during flight is possible in modern fly-by-wire aircraft by adding a sine sweep or pulse signal to the command signal sent to the primary control surfaces. However, during the actual flight, other excitation sources such as turbulence are present. Moreover, sticks inputs and minimum control laws are still active during the excitation and can also generate not controlled excitation. Sometimes, this results in rather noisy FRFs. For example, an aircraft tail response sensor receives a rather limited contribution from the wing excitation. Therefore the idea arose to neglect the excitation signal and apply Operational Modal Analysis to the aircraft acceleration signal. A similar reasoning applies to wind tunnel testing of scale models. The observation that the generated wind is exciting the model well above the noise floor of modern instrumentation and the practical challenges in providing measurable artificial excitation during wind tunnel testing lead to an interest in the use of Operational Modal Analysis.

The paper is organized as follows. In Section 2, the LMS PolyMAX method for Operational Modal Analysis (OMA) is reviewed. In Section 3, two case studies are discussed: one case combining 4 acceleration and 4 strain sensors mounted on an aircraft component and the second case involving 16 accelerometers mounted on an entire aircraft model. The 1st case study allows assessing the possibility to include strain measurements in the identification process and the 2nd case allows assessing the quality of the identified mode shapes. In both cases the performance and efficiency of automated tracking of the modal parameters during wind tunnel testing will be investigated.

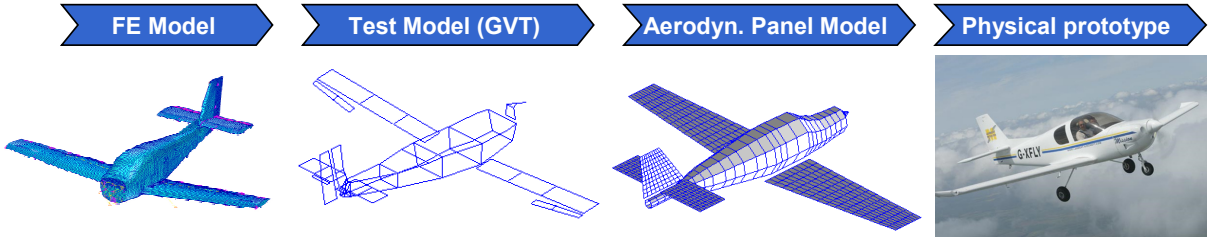

Figure 1: Aeroelasticity-related modelling and testing.

2. PolyMAX for Operational Modal Analysis

The estimation of eigenfrequencies, damping ratios and mode shapes from output-only vibration measurements is referred to as "Operational Modal Analysis" (OMA). Typical for the output-only case is that the lack of knowledge of the input is justified by the assumption that the input does not contain any information; or in other words, the input is white noise. The theoretical assumption of white noise turns out to be not too strict in practical applications. As long as the (unknown) input spectrum is quite flat, OMA methods will work fine. An overview and comparison of operational modal parameter estimation methods can be found in [6]. In this section, it will be discussed how the PolyMAX method, a particular algorithm which is very successful in classical modal analysis [7], can be used as well for Operational Modal Analysis.

2.1 Output-only frequency-domain model

Frequency-domain Operational Modal Analysis methods, such as PolyMAX, require output spectra as primary data. In this subsection, it will be shown that, under the assumption of white noise input, output spectra can be modelled in a very similar way as Frequency Response Functions (FRFs). It is well known that the modal decomposition of an FRF matrix $[H(\omega)] \in \mathbb{C}^{l \times m}$ is [8][9]:

$$[H(\omega)] = \sum_{i=1}^{n} \frac{\{v_i\} < l_i^T >}{j\omega - \lambda_i} + \frac{\{v_i^*\} < l_i^H >}{j\omega - \lambda_i^*} \tag{1}$$

where l is the number of outputs; m is the number of inputs; n is the number of complex conjugated mode pairs; $\bullet^*$ is the complex conjugate of a matrix; $\bullet^H$ is the complex conjugate transpose (Hermitian) of a matrix; $\{v_i\} \in \mathbb{C}^l$ are the mode shapes; $< l_i^T > \in \mathbb{C}^m$ are the modal participation factors and λ_i are the poles, which are related to the eigenfrequencies ω_i and damping ratios ξ_i as follows:

$$\lambda_i, \lambda_i^* = -\xi_i \omega_i \pm j\sqrt{1-\xi_i^2}\,\omega_i \tag{2}$$

The input spectra $[S_{uu}] \in \mathbb{C}^{m \times m}$ and output spectra $[S_{yy}(\omega)] \in \mathbb{C}^{l \times l}$ of a system represented by the FRF matrix $[H(\omega)]$ are related as:

$$[S_{yy}(\omega)] = [H(\omega)][S_{uu}][H(\omega)]^H \tag{3}$$

In case of operational data the output spectra are the only available information. The deterministic knowledge of the input is replaced by the assumption that the input is white noise. A property of white noise is that it has a constant power spectrum. Hence $[S_{uu}]$ in (3) is independent of the frequency ω. The modal decomposition of the output spectrum matrix is obtained by inserting (1) into (3) and converting to the partial fraction form [10][11]:

$$[S_{yy}(\omega)] = \sum_{i=1}^{n} \frac{\{v_i\} < g_i >}{j\omega - \lambda_i} + \frac{\{v_i^*\} < g_i^* >}{j\omega - \lambda_i^*} + \frac{\{g_i\} < v_i >}{-j\omega - \lambda_i} + \frac{\{g_i^*\} < v_i^* >}{-j\omega - \lambda_i^*} \tag{4}$$

where $< g_i > \in \mathbb{C}^l$ are the so-called *operational reference factors*, which replace the modal participation factors in case of output-only data. Their physical interpretation is less obvious as they are a function of all modal parameters of the system and the constant input spectrum matrix. Note that the order of the power spectrum model is twice the order of the FRF model. The goal of OMA is to identify the right hand side terms of (4) based on measured output data pre-processed into output spectra (Section 0).

2.2 Pre-processing operational data

Power spectra are defined as the Fourier transform of the correlation sequences. The most popular non-parametric spectrum estimate is the so-called *weighted averaged periodogram* (also known as *modified Welch's periodogram*). Weighting means that the signal is weighted by one of the classical windows (Hanning, Hamming, …) to reduce leakage. Welch's method starts with computing the discrete Fourier transform (DFT) $Y(\omega) \in \mathbb{C}^l$ of the weighted outputs:

$$Y(\omega) = \sum_{k=0}^{N-1} w_k y_k \exp(-j\omega k\Delta t) \tag{5}$$

where $y_k \in \mathbb{R}^l$ is the sampled output vector (the measurements); w_k denotes the time window; k is the time instant; N the number of time samples and Δt the sampling time. An unbiased estimate of the spectrum is the weighted periodogram:

$$S_{yy}^{(b)}(\omega) = \frac{1}{\sum_{k=0}^{N-1} |w_k|^2} Y(\omega) Y^H(\omega) \tag{6}$$

The variance of the estimate is reduced by splitting the signal in possibly overlapping blocks, computing the weighted periodogram of all blocks and taking the average:

$$S_{yy}(\omega) = \frac{1}{P} \sum_{b=1}^{P} S_{yy}^{(b)}(\omega) \tag{7}$$

where P is the number of blocks and superindex b denotes the block index.

Another non-parametric spectrum estimate is the so-called *weighted correlogram*. It will be shown that this estimate has some specific advantages in a modal analysis context. First the correlation sequence has to be estimated (i being the *time lag*):

$$R_i = \frac{1}{N} \sum_{k=0}^{N-1} y_{k+i} y_k^T \tag{8}$$

High-speed (FFT-based) implementations exist to compute the correlations as in (8); see for instance [12]. The weighted correlogram is the DFT of the weighted estimated correlation sequence:

$$S_{yy}(\omega) = \sum_{k=-L}^{L} w_k R_k \exp(-j\omega k\Delta t) \tag{9}$$

where L is the maximum number of time lags at which the correlations are estimated. This number is typically much smaller than the number of data samples to avoid the greater statistical variance associated with the higher lags of the correlation estimates. In a modal analysis context, the weighted correlogram has the following advantages:

It is sufficient to compute the so-called *half spectra* which are obtained by using only the correlations having a positive time lag in (9):

$$S_{yy}^{+}(\omega) = \frac{w_0 R_0}{2} + \sum_{k=1}^{L} w_k R_k \exp(-j\omega k\Delta t) \tag{10}$$

The relation between the half spectra (10) and the full spectra (9) is the following:

$$S_{yy}(\omega) = S_{yy}^{+}(\omega) + \left(S_{yy}^{+}(\omega)\right)^H \tag{11}$$

It can be shown (see for instance [10]) that the modal decomposition of these half spectra only consists of the first two terms in (4):

$$S_{yy}^{+}(\omega) = \sum_{i=1}^{n} \frac{\{v_i\} < g_i >}{j\omega - \lambda_i} + \frac{\{v_i^*\} < g_i^* >}{j\omega - \lambda_i^*} \tag{12}$$

The advantage in modal analysis is that models of lower order can be fitted without affecting the quality.

Under the white noise input assumption, the output correlations are equivalent to impulse response. So, just like in impact testing, it seems logical to apply an exponential window w_k to the correlations before computing the DFT (10). The exponential window reduces the effect of leakage and the influence of the higher time lags, which have a larger variance. Moreover, the application of an exponential window to impulse responses or correlations is

compatible with the modal model and the pole estimates can be corrected. This is not the case when a Hanning window is used: such a window always leads to biased damping estimates.

2.3 PolyMAX modal parameter estimation

After having pre-processed output data into output spectra (Section 0), it is now the task to identify a modal model (Section 0). By comparing (12) with (1), it is clear that FRFs and half spectra can be parameterised in exactly the same way. By consequence, the same modal parameter estimation methods can be used in both cases. The PolyMAX frequency-domain system identification method considered in this paper identifies in a first step following so-called right matrix-fraction model:

$$[H(\omega)] = \sum_{r=0}^{p} z^r [\beta_r] . \left(\sum_{r=0}^{p} z^r [\alpha_r] \right)^{-1} \tag{13}$$

where $H(\omega) \in \mathbb{C}^{l \times m}$ is the Frequency Response Function (FRF) matrix that is estimated in a non-parametric way from the measured vibration data; for output-only data the FRF is substituted by the half-spectrum matrix (12); $[\beta_r] \in \mathbb{R}^{l \times m}$ are the numerator matrix polynomial coefficients; $[\alpha_r] \in \mathbb{R}^{m \times m}$ are the denominator matrix polynomial coefficients; l is the number of outputs; m is the number of inputs; p is the model order. Note that a so-called z-domain model (i.e. a frequency-domain model that is derived from a discrete-time model) is used in (13), with $z = \exp(j\omega\Delta t)$ and Δt being the sampling time. In modal analysis applications, the right matrix fraction model (13) is, after identification, analytically converted to a modal model: (1) or (12).

Different procedures exist to identify a right matrix fraction model from measured FRFs. Equation (13) can be written down for all values ω of the frequency axis of the FRFs. Basically, the unknown model coefficients $[\alpha_r], [\beta_r]$ can be found as the Least-Squares (LS) solution of these equations after linearization. The PolyMAX algorithm is such a LS implementation which has been memory and time optimized and uses a particular parameter constraint. More details about the PolyMAX method can be found in [7][13]. Mainly due its user-friendliness (the method yields extremely clear stabilization diagrams), PolyMAX is considered as an important breakthrough in modal parameter estimation. The method is both implemented as part of the standard LMS Test.Lab software suite [14] as the dedicated Flutter Analysis package [15].

3. Case studies

3.1 Wind tunnel test combining strain and acceleration data

In a first case study, 4 accelerometers and 4 strain gauges were mounted on a wind tunnel test model. These data allow verifying the possibility to use both quantities in a flutter detection scheme. Figure 2 gives an overview of the entire test. It shows the Mach number and segments of strain measurements at constant Mach numbers.

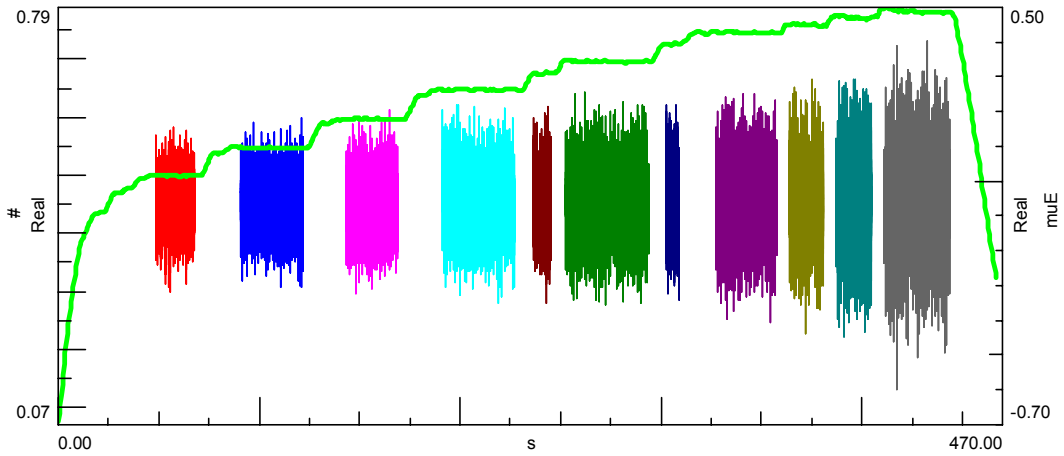

Figure 2: Mach number and segments of strain measurements at constant Mach numbers.

Figure 3 (Left) shows the power spectra of the acceleration and strain signals at a constant Mach number. Based on the inspection of these power spectra, the 3rd acceleration signal (Blue) and the 4th strain gauge signal (Dark Blue) were selected as references. Both signals have large amplitudes and seem to contain most of the dynamics (i.e. many

peaks present). Reference sensors play an important role in OMA since the cross spectra computations (12) are typically restricted to a rectangular matrix that contain the cross spectra between all sensors and a limited set of references. It is therefore important that good-quality signals are selected. Figure 3 (Right) shows stabilization diagrams obtained when applying PolyMAX to acceleration and strain signals respectively. It is clear that to a large amount the same modes are extracted in both cases. The identified eigenfrequencies and damping ratios are listed in Table 1. Also from these numbers, the good match of identification results is obvious. Figure 4 compares measured spectra with spectra synthesized from the identified modal parameters; i.e. right hand side of (12).

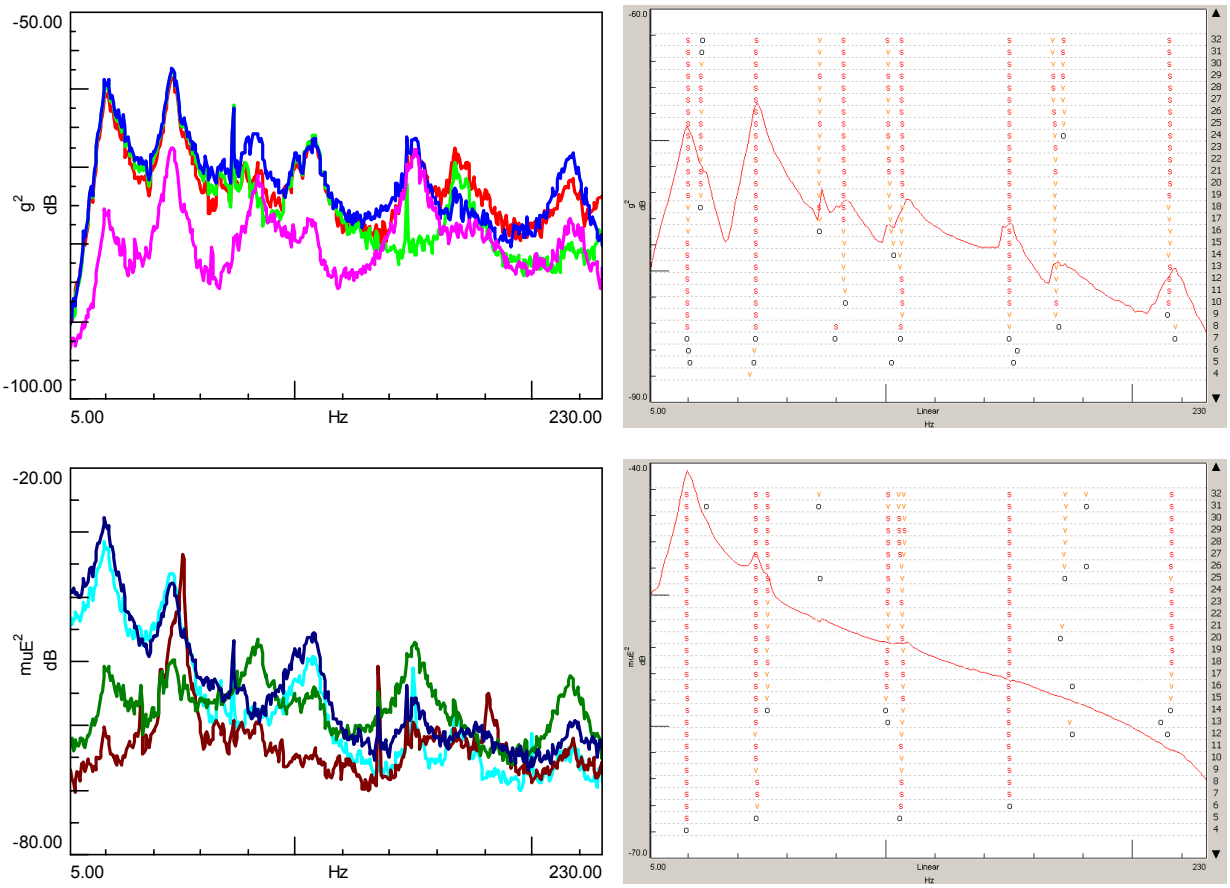

Figure 3: (Left) Power spectra of signals at constant Mach number; (Right) PolyMAX stabilization diagrams; (Top) using only acceleration signals; (Bottom) using only strain signals.

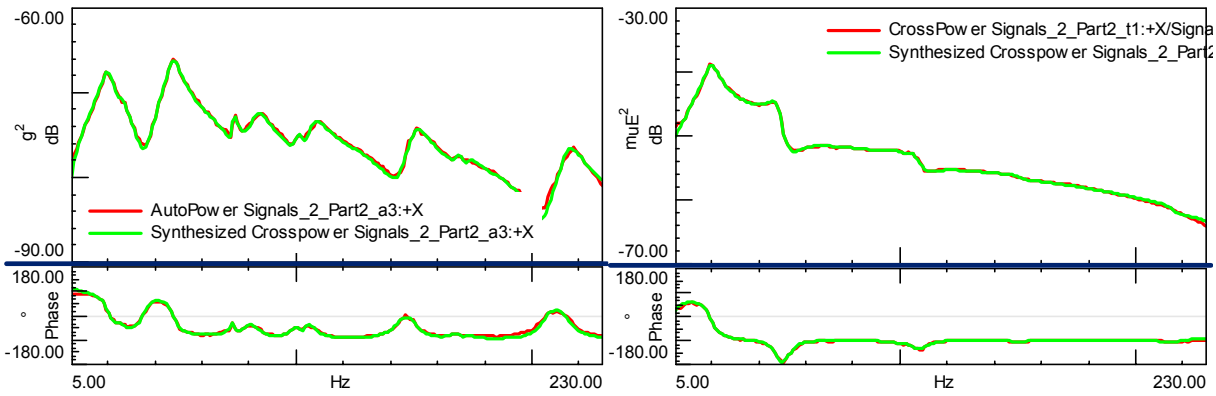

Figure 4: Comparison between measured (Red) spectra and synthesized spectra (Green). (Left) acceleration data; (Right) strain data.

Table 1: Identified eigenfrequencies and damping ratios from different measurement quantities: using only acceleration signals, using only strain signals, and using both types of signals.

Mode (i)	Acceleration data		Strain data		Combined data	
	f_i [Hz]	ξ_i [%]	f_i [Hz]	ξ_i [%]	f_i [Hz]	ξ_i [%]
1	20.13	11	19.75	11	19.76	9.4
2	47.69	4.3	47.76	4.3	47.96	4.1
3	106.7	2.9	106.7	3.4	107.5	2.1
4	150.5	2.2	150.4	2.3	150.6	2.2
5	215.7	1.7	216.2	1.7	215.8	1.6

As discussed earlier in this paper, the main advantage of PolyMAX is that it yields extremely clear stabilisation diagrams. This makes an automation of the parameter identification process rather straightforward and enables a continuous monitoring of the dynamic properties of a structure. An overview and discussion on automatic modal analysis techniques can be found in [16]. Automated modal analysis is still an active field of research. For instance, in [17], an interesting new approach is presented that is based on clustering techniques that does not require any user-specified parameter or threshold value.

Unlike above, no attempts were made to isolate certain data segments at constant Mach number, but the data were simply continuously analysed using a sliding window approach. Independent, automated modal analyses were applied to these highly-overlapping windows. Figure 5 shows the automatic PolyMAX results. The diagram is very clean and 6 modes can be easily tracked. For some of the modes there is a clear dependency of the eigenfrequencies on the data block number and thus measurement instant and thus Mach number. Some investigations were performed related to the minimal length of the time window in the continuous tracking. This minimal length is expected to be related to the frequency of the lowest mode of interest: to have a good identification of a mode, a sufficient number of cycles should be present in the data. It was observed that data segments of 4 seconds still yielded good results. Combining this segment length with an overlap factor of 75% would represent a one second-update of the modal parameters, making use of the data of the last 4 seconds. Figure 6 shows the tracking of 2 modes based on Figure 5. The mode around 20 Hz increases in frequency and after an initial increase of damping, shows a decrease with increasing Mach number. The mode around 150 Hz shows a decrease in frequency and an increase in damping. Finally, Figure 7 shows the tracking of the 3 lowest modes at 7 discrete points with constant Mach number. These 7 points correspond to the 7 longest segments indicated in Figure 7. The lowest mode in this figure (blue line) was also represented in the continuous tracking (Figure 6) where it showed a similar trend.

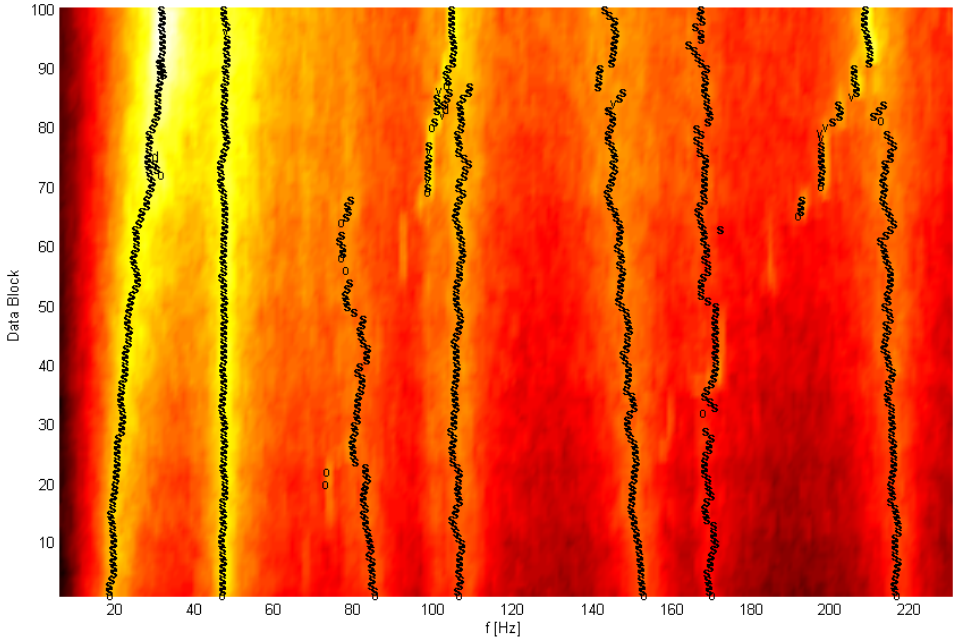

Figure 5: Automatic modal analysis results: the y-axis represents the index to the sliding window time segment that was used in the analysis; the x-axis is the frequency axis with an indication of identified poles. Each data segments is about 16 s long and overlaps 75% with the previous.

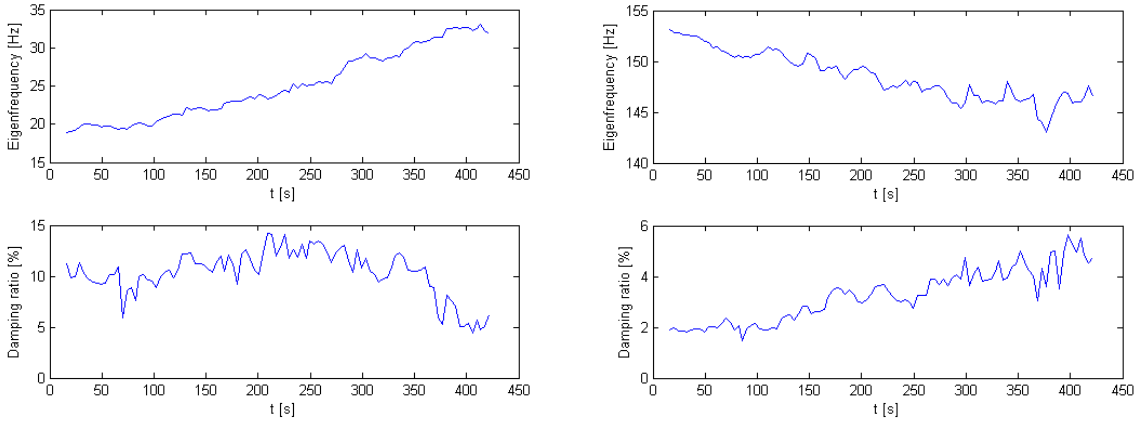

Figure 6: Continuous tracking results of eigenfrequencies (Top) and damping ratios (Bottom) of Mode around 20 Hz (Left) and Mode around 150 Hz (Right).

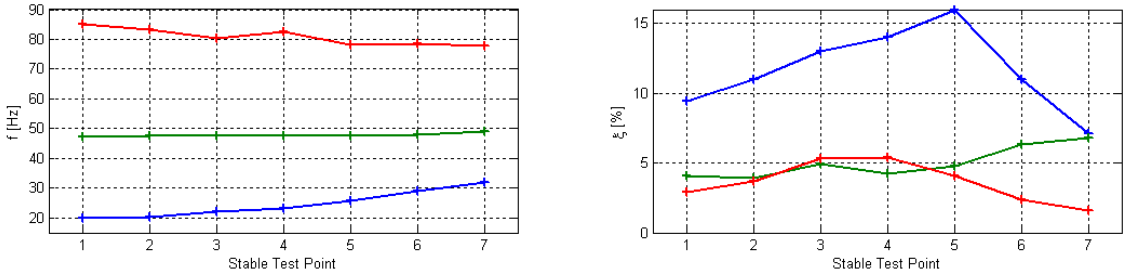

Figure 7: Discrete tracking of modes using data segments at constant Mach number. (Left) eigenfrequeencies; (Right) damping ratios of the 3 lowest modes.

3.2 Wind tunnel test with relatively large number of accelerometers

Interesting about this case is that 16 accelerometers were mounted on an aircraft scale model, allowing the visualization of the measured mode shapes. During the test that had a duration of about 500 s, the wind speed was gradually increased. During 4 stages, the wind speed was kept constant (scaled wind speed of 0.70, 0.78, 0.88, 1.00) and an additional impact excitation was applied (See Figure 8: high amplitude spike accelerations during constant wind speeds).

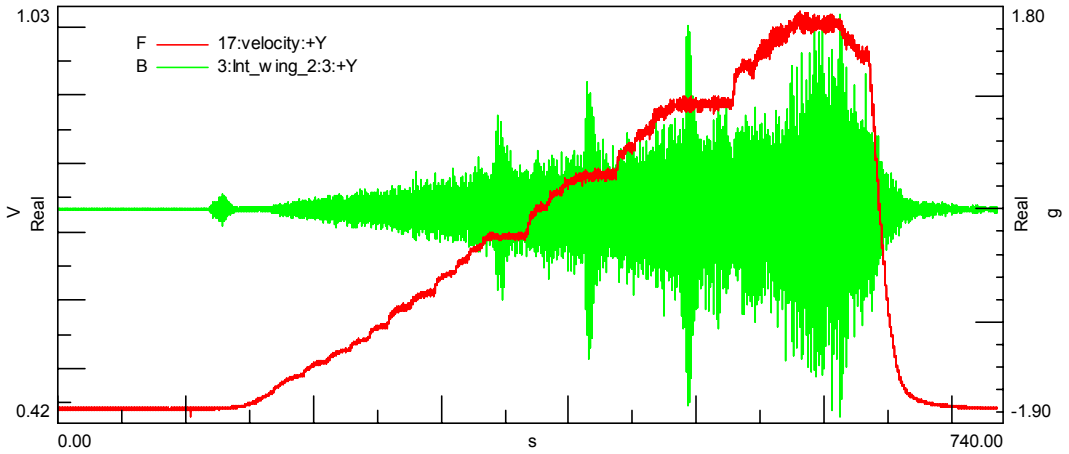

Figure 8: Wind speed (scaled) and typical acceleration signal.

Just like in the previous case study (Section 0), the reference sensors were selected by comparing the power spectra of all signals (Figure 9 – Left). To capture both vertical and horizontal modes, at least one reference sensor was selected in both directions. In addition, the wing tip sensors appeared to be good candidates ((Figure 9 – Right). Figure 10 shows the evolution of some of the power spectra with increasing wind speeds at the 4 constant wind speed segments. It is clear that the amplitudes increase with increasing wind speed, but the change in location of the resonance peaks is less apparent. These changes can be highlighted by applying OMA to the data. Figure 11 shows the eigenfrequencies and damping ratios of 9 modes identified with PolyMAX as a function of wind speed. Figure 12 shows some typical bending and torsion mode shapes.

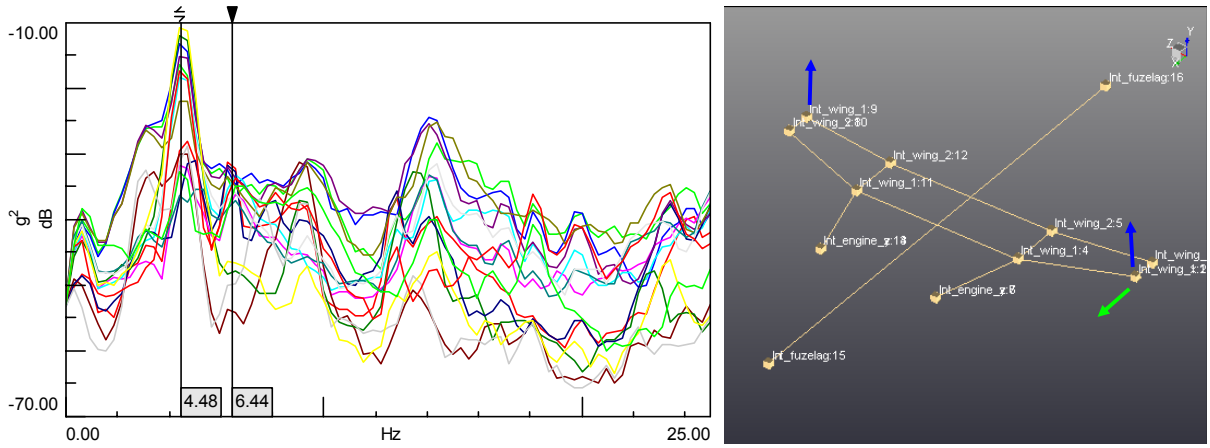

Figure 9: (Left) Power spectra at constant wind speed data segment. The left cursor indicates vertical mode and the right cursor a horizontal one; (Right) sensor locations and indication of reference sensors.

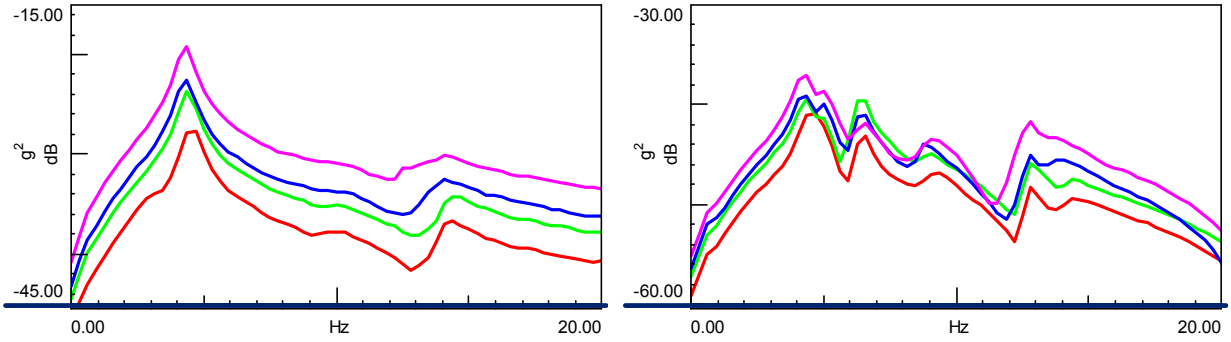

Figure 10: Evolution of power spectra at increasing wind speeds (red – green – blue – pink). (Left) vertical wing tip sensors; (Right) horizontal wing tip sensor.

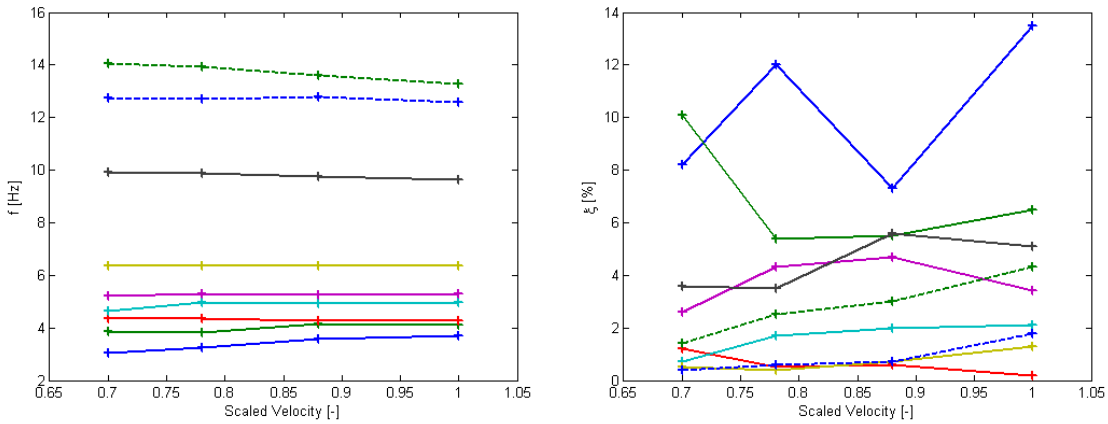

Figure 11: Discrete tracking of modes using data segments at constant wind speed. (Left) eigenfrequeencies; (Right) damping ratios.

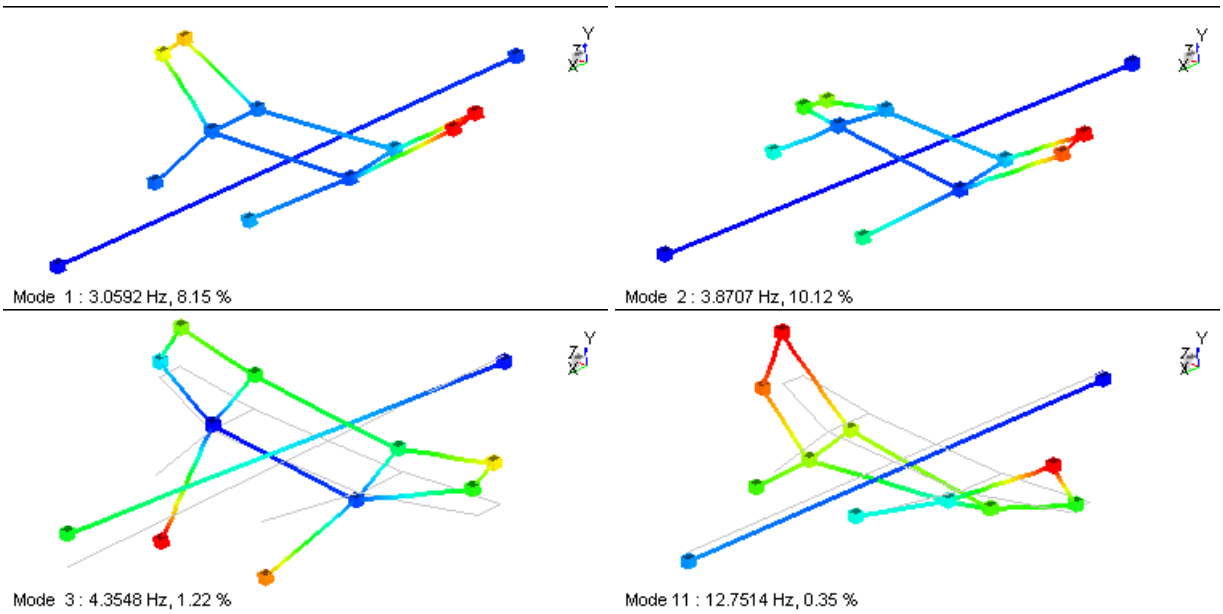

Figure 12: Mode shapes identified with OMA-PolyMAX using wind tunnel data.

Finally, also an automated modal analysis was applied to highly-overlapping windows selected from the entire data set (Figure 13). Quite some modes can be tracked. Interesting to note is that when the additional impact excitation is applied (areas of constant wind velocity and high spectral amplitudes in Figure 13), an additional mode is found around 4.3 Hz. It was observed that data segments of 30 s still yielded good results. Combining this segment length with an overlap factor of 95% would represent an update of the modal parameters at 1.5 s, making use of the data of the last 30 s. The need for 30 s of data to make reliable estimates may seem long, but considering the fact that the lowest mode is around 3 Hz, the time segment only contains 100 periods of the lowest mode.

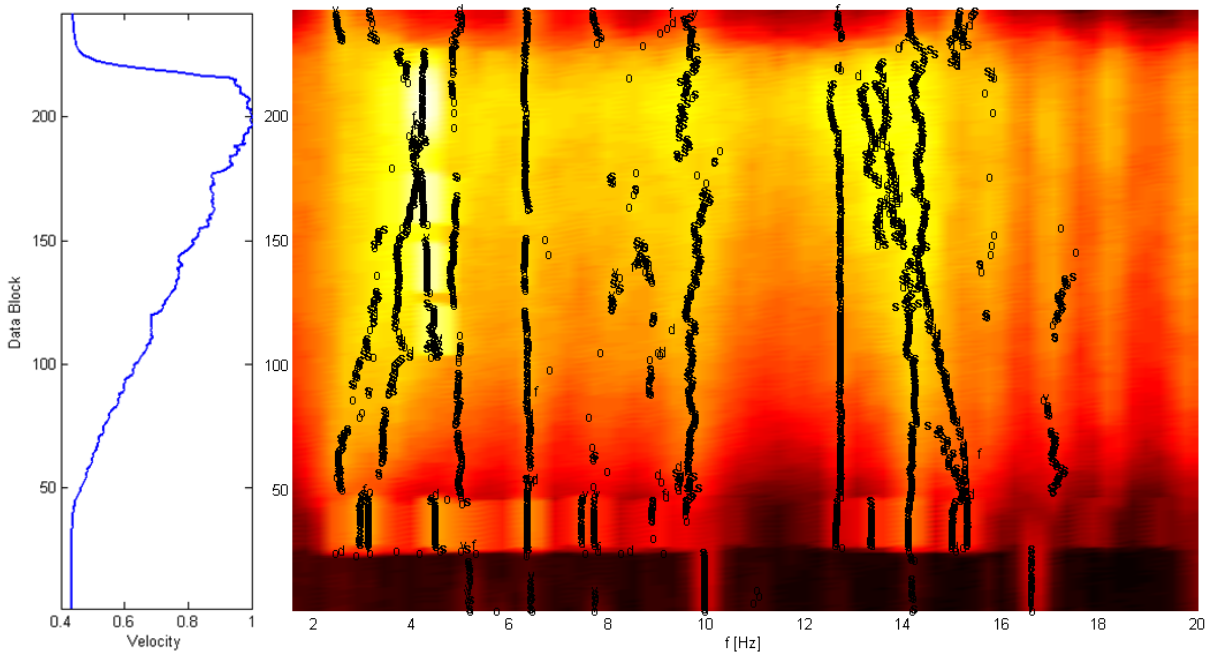

Figure 13: Automatic modal analysis results: the y-axis represents the index to the sliding window time segment that was used in the analysis; the x-axis is the frequency axis with an indication of identified poles. Each data segments is about 60 s long and overlaps 95% with the previous. The curves on the Left represent the wind speed at the different estimations.

4. Conclusions

This paper discussed the application of (automated) Operational Modal Analysis for in-line flutter assessment during wind tunnel testing of scaled models. Two case studies were considered: one case combining 4 acceleration and 4 strain sensors mounted on an aircraft component and the second case involving 16 accelerometers mounted on an entire aircraft model. It was found that the PolyMAX method for OMA could successfully identify the modes from the output-only data. The excitation forces could not be measured as they originated from the wind itself. In the 2nd case study it was observed that applying an additional impact excitation did not improve dramatically the identification of most of the modes, although it was found that 1 additional mode appeared in the data. Other observations are that also strains can be successfully used to estimate the eigenfrequencies and damping ratios and if a sufficient number of accelerometers are available, high-quality mode shapes can also be estimated. Finally, the performance and efficiency of continuous tracking were investigated. It was found that it is possible to obtain each second an update of the estimates. This update rate depends on the overlapping factor and is limited by the calculation time needed in the PolyMAX algorithm. Evidently, these updates can only be obtained by analysing a sufficient amount of "historical" data. The needed time window depends on the lowest mode and as a rule of thumb, it seems that around 100 cycles of the lowest-frequency mode are required to obtain accurate estimates. In the 1st case study, about 4 s of data were needed (lowest frequency = 20 Hz) and in the 2nd case study, about 30 s of data were needed (lowest frequency = 3 Hz).

References

[1] KEHOE, M.W. *A historical overview of flight flutter testing*. NASA technical memorandum 4720, 1995.

[2] PICKREL, C.R., WHITE, P.J. Flight flutter testing of transport aircraft: in-flight modal analysis. In *Proceedings of IMAC 21, the International Modal Analysis Conference*, Kissimmee (FL), USA, 2003.

[3] ZIMMERMAN, N.H., WEISSENBURGER, J.T. Prediction of flutter onset speed based on flight testing at subcritical speeds. *Journal of Aircraft*, **1**(4):190-202, 1964.

[4] LIND, R. Flight-test evaluation of flutter prediction methods. *Journal of Aircraft*, **40**(5):964–970, 2003.

[5] DE TROYER, T., ZOUARI, R., GUILLAUME, P., MEVEL, L. A new frequency-domain flutter speed prediction algorithm using a simplified linear aeroelastic model. In *Proceedings of the ISMA 2008 International Conference on Noise and Vibration Engineering*, Leuven, Belgium, 2008.

[6] PEETERS, B., DE ROECK, G. Stochastic system identification for operational modal analysis: a review. *ASME Journal of Dynamic Systems, Measurement, and Control*, **123**(4):659-667, 2001.

[7] PEETERS, B., VAN DER AUWERAER, H., GUILLAUME, P., LEURIDAN, J. The PolyMAX frequency-domain method: a new standard for modal parameter estimation? *Shock and Vibration*, **11**:395–409, 2004.

[8] EWINS, D.J. *Modal Testing: Theory, Practice and Application*. Research Studies Press, Baldock, Hertfordshire, UK, 2000.

[9] HEYLEN, W., LAMMENS, S., SAS, P. *Modal Analysis Theory and Testing*. K.U.Leuven, Belgium, 1997.

[10] HERMANS, L, VAN DER AUWERAER, H. GUILLAUME, P. A frequency-domain maximum likelihood approach for the extraction of modal parameters from output-only data. In *Proceedings of ISMA23, the International Conference on Noise and Vibration Engineering*, Leuven, Belgium, 1998.

[11] HERMANS, L., VAN DER AUWERAER, H. Modal testing and analysis of structures under operational conditions: industrial applications. *Mechanical Systems and Signal Processing*, **13**(2):193–216, 1999.

[12] OPPENHEIM, A.V., SCHAFER, R.W. *Digital Signal Processing*. Prentice-Hall, 1975.

[13] PEETERS, B., VAN DER AUWERAER, H., VANHOLLEBEKE, F., GUILLAUME, P. Operational modal analysis for estimating the dynamic properties of a stadium structure during a football game. *Shock and Vibration*, **14**(4):283-303, 2007.

[14] LMS INTERNATIONAL. LMS Test.Lab, www.lmsintl.com, Leuven, Belgium, 2011.

[15] LANSLOTS, J., DEBILLE, J., LEPAGE, A., NAUDIN, P., PEETERS, B. Industrial solutions for in-flight & offline experimental flutter analysis. In *Proceedings of IFASD 2009, the International Forum on Aeroelasticity and Structural Dynamics*, Seattle (WA), USA, 2009.

[16] VAN DER AUWERAER, H., PEETERS, B. Discriminating physical poles from mathematical poles in high order systems: use and automation of the stabilization diagram. In *Proceedings of IMTC 2004, the IEEE Instrumentation and Measurement Technology Conference*, Como, Italy, 2004.

[17] REYNDERS, E., HOUBRECHTS, J., DE ROECK, G. Automated interpretation of stability diagrams. In *Proceedings of IMAC 29, the International Modal Analysis Conference*, Jacksonville (FL), USA, 2011.